Peer-reviewed version available at Machines 2017, 5, 32; doi:10.3390/machines5040032

*Article*

# A moving 3D laser scanner for automated underbridge inspection

**Marco Tarabini[1*], Hermes Giberti[2], Silvio Giancola[1], Matteo Sgrenzaroli[3], Remo Sala[1], Federico Cheli[1].**

[1] Politecnico di Milano, Dipartimento di Meccanica, Via La Masa 1, Milano, Italy
[2] Università degli Studi di Pavia, Dipartimento di Ingegneria Industriale e dell'Informazione, via Ferrata 5, 27100, Pavia, Italy.
[3] Gexcel - Geomatics & Excellence, Via Branze 45 - 25123 Brescia, Italy
* Correspondence: marco.tarabini@polimi.it; Tel.: +39-02-2399-8808

**Abstract:** Recent researches proved that the underbridge geometry can be reconstructed by mounting a 3D laser scanner on a motorized cart travelling on a walkway located under the bridge. The walkway is moved by a truck and the accuracy of the bridge model depends on the accuracy of the trajectory of the scanning head with respect to a fixed reference system. In this paper, we describe the metrological characterization of a method that uses non-contact systems to identify the relative motion of the cart with respect to the walkway; the orientation of the walkway with respect to the bridge is determined using inclinometers and optical rails, while the position of the truck with respect to the bridge is measured using a conventional odometer. The measurement uncertainty of the proposed system was initially evaluated by numerical simulations and successively verified by experiments in laboratory conditions. The complete system has then been tested in operative conditions; the validity of the proposed approach has been demonstrated by comparing the geometry of buildings reconstructed with the proposed system with the geometry obtained with a static scan. Results evidenced that the errors are approximately 6 mm.

**Keywords:** laser; construction monitoring; measurements; uncertainty; bridge inspection

## 1. Introduction

The automation of bridge inspections is the focal point of several studies [1-7], given that many existing highway bridges were built in the 60s [1] and the inspection procedures are becoming extremely expensive [2]. The visual inspection of concrete bridges performed by skilled technicians has different limitations generated by the discretional margins in the identification of the concrete defects. According to McCrea et al. [3], metallic bridges are typically monitored using non-destructive techniques while concrete bridges are mainly monitored using visual analyses, given the difficulty of creating inspection systems capable of detecting defects of a few millimetres on constructions of hundreds of meters. One of the most promising techniques is the analysis of images as proposed by Yu et al. [7], but great limitations derive from the difficulty in associating the exact position to each image; despite different works [8-10] focused on the methods for managing the huge amount of data deriving from image analysis, these methods do not provide any geometrical information about the bridge.

The idea of using a moving laser scanner to reconstruct the underbridge geometry has been proposed and validated [1,2], but the accuracy of the reconstruction was not sufficient, with geometrical errors of approximately ±70 mm. The main source of error was the large uncertainty in the reconstruction of the scanning head trajectory and orientation; in the literature, the objects' egomotion has been measured with several different approaches [11-16] and the technique that grew more rapidly is the Visual Odometry (VO) [11], the process in which the motion of a vehicle (or subject) is detected starting from the images acquired by a single or multiple cameras. The estimation of a vehicle motion from images was pioneered by Moravec in the 1980s [16] and the term VO was

Preprints (www.preprints.org) | NOT PEER-REVIEWED | Posted: 27 October 2017 doi:10.20944/preprints201710.0172.v1

Peer-reviewed version available at Machines 2017, 5, 32; doi:10.3390/machines5040032



introduced in 2004 by Nister thanks to the similarity to wheel odometry, which incrementally estimates the motion of a vehicle by integrating a wheel rotation [11,15]. As outlined by Scaramuzza and Fraundorfer in their review on VO [15], the technique is effective only if there is sufficient illumination in the environment and the static scene has enough features to allow the identification of the relative motion; the framerate has to be large enough to allow the images overlap. VO can provide relative position error ranging from 0.1 to 2%. This capability makes VO an interesting alternative to the conventionally used techniques (global positioning system, inertial measurement units, and laser odometry). The early VO studies were motivated by the NASA Mars exploration program to measure the rovers' motion and, in general, this technique is the preferred choice in environments where the global positioning system is not available or does not provide for the required accuracy.

The present study was developed to identify the position of a cart moving on the walking platform of a bridge inspection truck, as shown in Figure 1. The cart is equipped with a 3D laser scanner used to reconstruct a 3D map of the underbridge using a helical scan. The mathematical formulation of the problem and the preliminary experimental results were presented in references [1,2,17,18]. The accuracy in the reconstruction of the underbridge geometry (cloud of points) obtained in the tests was limited, mainly because of the limited accuracy of the system used to identify the position of the cart on the walkway, which was based on the hypothesis of small cart roll, pitch and yaw.

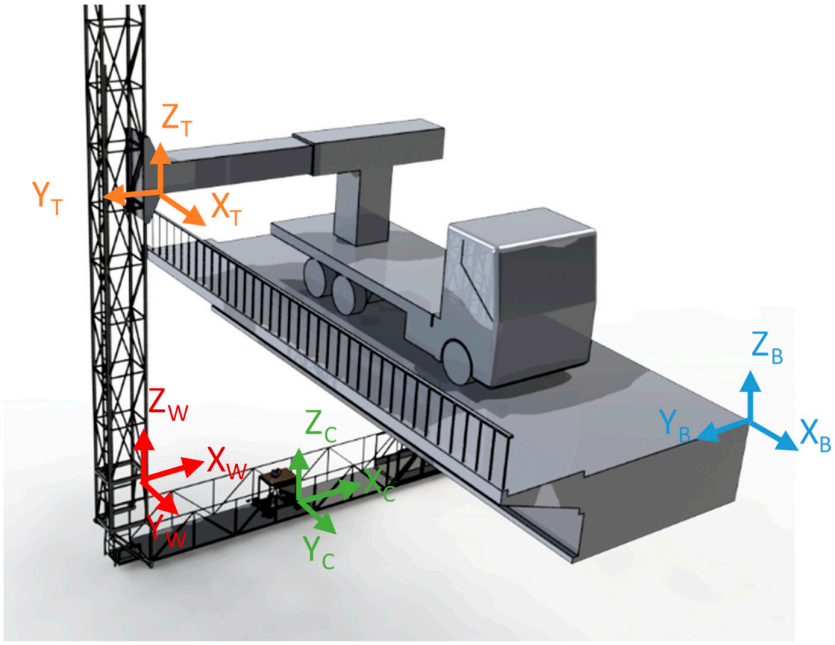


**Figure 1** Scheme of the cart moving on the by-bridge walkway

The system used to identify the relative position between the cart reference system (with subscript C in Figure 1) and the origin of the by-bridge walkway (with subscript W in Figure 1) was described in ref. [17], while the relative positions between the bridge reference system (subscript B), the truck reference system (subscript T) and the walkway reference systems will be identified with the methods described in this paper. Additionally, the position of a laser scanner placed over the cart was estimated calculating the relative position of the laser head relative to the cart (boresight operation), to determine the position of the laser scanner used to acquire 3D Points in helical mode. Different issues prevented the adoption of existing techniques:

- GPS cannot be used because of the limited accuracy and because of the poor signal quality on the surface immediately below the bridge deck;
- The classical VO can fail because of the lack of features of the surrounding environment (flat underbridge), non-controlled environment.

Peer-reviewed version available at Machines 2017, 5, 32; doi:10.3390/machines5040032



- Inertial Measurement Units were the baseline solution at the beginning of the project, but the long measurement duration induced relevant drift problems;
- The use of the encoder-based odometer for the identification of the cart position lead to poor results because of the wheels' slippage;
- Vision systems for the measurement of cart position (pattern matching techniques to track the position of the cart using fixed cameras or trinocular stereoscopic systems using markers) were also viable solutions; the worsening accuracy of 3D reconstruction at the increasing distances evidenced in tests performed in controlled conditions [19] was not acceptable for our application.

Simultaneous Localization and Mapping (SLAM) techniques focusing on the cart position on the walkway is difficult to implement because the relative motion between the cart, the walkway, the truck frame, and the bridge implies that different parts of the images are moving in different directions.

The problem was solved by developing a custom system entirely based on noncontact techniques, given the positive results evidenced numerical simulations. The breakdown of the uncertainty budget (identified with the technique described in ref. [20]) evidenced the necessity of considering the nonlinear terms in the rotation matrices, given that the linearization-induced errors were close to 20 mm. The effects of the tilt uncertainties were generally larger than those of uncertainties in distance measurements. Laboratory experiments permitted validating the entire measurement procedure, which involved also the conversion of raw data acquired by the Faro 3D scanning head into a cloud of points. The RMS of the planarity error was 6 mm, a value three times smaller than that obtained with the previous configuration.

## 2. Method

The position of the scanning head can be identified applying roto-translations starting from the position of the truck:

$$M_{0N} = M_{01}M_{12}M_{23} \dots M_{(N-1)N}$$

Where

$$[M_{01}] = \begin{bmatrix} R_{01} & T_{01} \\ 0 & 1 \end{bmatrix}$$

R01 and T01 are respectively the rotation matrix (3x3) and the translation vector (3x1) which describe the position of a reference system with respect to the previous one. The rotation matrix R cannot be linearized and the rotations:

$$R_{01} = \begin{bmatrix} 1 & -\gamma & \beta \\ \gamma & 1 & -\alpha \\ -\beta & \alpha & 1 \end{bmatrix}$$

The system that measures the cart position with respect to the walkway is set-up with:

- a laser distance meter and two laser pointers located at the beginning of the by-bridge walkway;
- a camera on the cart which observes the three spots on the projection plane;
- two cameras on the cart observing sideward and downwards; and
- an encoder for the closed-loop control of the cart motor

The scheme of the measurement chain is shown in Figure 2; the three laser beams generate three spots on the projection plane; the central one is the laser distance meter, while the other two are used as optical rails. The three lasers are aligned with the cart motion direction, so that the displacement of the three points on the projection plane is limited. The downward and the lateral cameras observe respectively a metering tape fixed to the walkway and the walkway handrail.

Preprints (www.preprints.org) | NOT PEER-REVIEWED | Posted: 27 October 2017 doi:10.20944/preprints201710.0172.v1

Peer-reviewed version available at Machines 2017, 5, 32; doi:10.3390/machines5040032



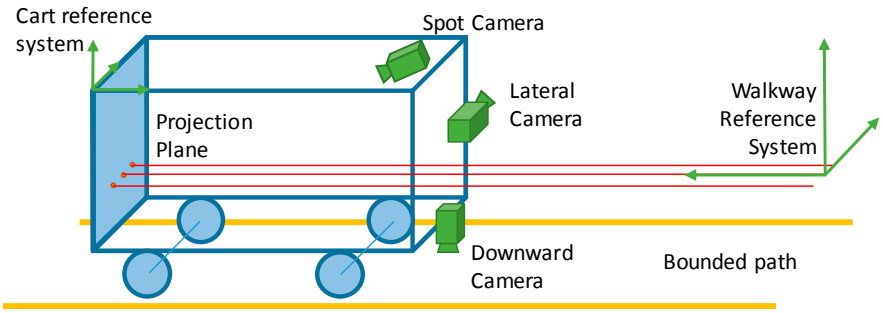


**Figure 2** Scheme of the measurement chain

With the proposed setup, the cart position is identified as follows:

- the fore-and-aft motion (XC in Figure 1) is determined by the laser range finder located at the beginning of the walkway;
- the lateral and vertical motion of the cart are measured by the spot camera, which identifies the translation from the position of the central spot;
- the cart roll is measured by the spot camera, observing the rotation of the two external laser spots
- the cart pitch and yaw are measured respectively by the lateral and the vertical cameras, observing linear objects parallel to the cart motion.

In the actual method implementation, there is no data fusion between the information of the different measurement systems: the lateral camera, for instance, can be used to identify also the vertical cart displacement but, at this initial stage, we decided to keep the method as simple as possible. As in any vision system, the quality of the image is crucial for obtaining reliable measurements. In our case, the biggest problem is probably related to the large variation of lighting and viewing condition of the scene, since at the beginning and at the end of the bridge the cameras may be exposed to the direct sunlight while below the bridge the lighting condition may be very poor.

Regarding the phase shift laser scanner, it was positioned over the cart. The laser scanner can work in two modes: i) spherical mode, and ii) helical mode. In the first mode, the laser scanner acquires the 3D coordinates of the visible points around the scanner head in a field of view of 310° (vertical) x 360° (horizontal).

In the second mode, the horizontal axe is fixed and the laser can acquire 310° vertical sections; the combination of the cart movement and the scanner vertical rotation guaranteed a 3D acquisition. To use the scanner in helical mode given the cart trajectory, the relative position between cart and laser scanner head must be determined; a boresight technique was used for this purpose. 4 targets detectable form the laser scanner were positioned jointly liable with the cart. The next paragraphs describe the measurement subsystems and the actions taken to obtain reliable measurements.

### *2.1. Experimental setup*

The three cameras used for the identification of the cart roll, pitch and yaw are manufactured by IDS (uEye UI-5240CP-M-GC); the image resolution is 1280x1024 pixels and the maximum frame rate is 25 Hz. A LabVIEW-based software running on an embedded PC captures the images, that are analyzed offline in order to tune the algorithms in case of non-standard lighting conditions.

#### 2.1.1. Laser pointers and Camera

The cart position along the X axis (direction of motion, almost perpendicular to the projection plane) is detected by the laser range finder (FAE LS121 FA, range 100 m, resolution 0.1 mm). The cart lateral and vertical motions (Y and Z axes in Figure 3(a)), as well as the cart roll are measured by analyzing the image captured by the camera. The translations are measured by the position of the central spot and the two external spots are used to identify the cart roll. The scheme of the measurement setup is shown in Figure 3.

Peer-reviewed version available at Machines 2017, 5, 32; doi:10.3390/machines5040032



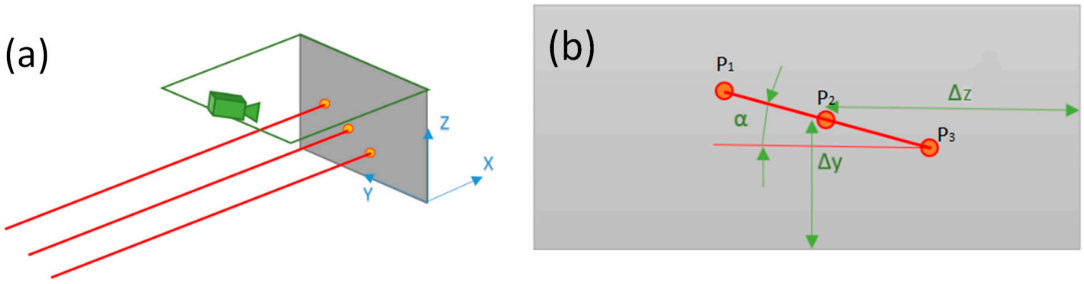


**Figure 3:** Laser spots on the projection plane (a) and scheme of the cart rotation measurement (b)

Since the camera sensor is not parallel to the observation plane, the system was calibrated by observing a grid with known geometry (diameter 6 mm, grid pitch 25 mm), so that the result of measurement is an array of spots coordinates in physical units. In order to obtain good images independently from the sunlight conditions, the camera deputed to observe the 3 spots has a bandpass filter from 635 to 646 nm, given that the three lasers have a wavelength of 639 nm (red color). The alignment between the three lasers strongly affects the measurement accuracy and consequently we developed a fit-to-purpose calibration procedure (described in section 2.2).

The coordinates of the three laser spots are identified using blob detection algorithm, based on a classical image thresholding paired by a blob analysis. The threshold level was set to 30 (8-bit grayscale image) and the lookup region of interest (ROI) is rearranged dynamically, since between an acquisition and the other the movement should not exceed 30 pixels. This value corresponds to a displacement lower than 15mm in 40 ms; the value was obtained with experiments performed by fixing an accelerometer on the cart and analyzing the maximum velocity. This procedure allowed a reduction of the image processing time, which is in the order of a few milliseconds per frame.

### 2.1.2. Lateral and Vertical camera

The vertical camera was located in order to observe a roller meter below the cart; also in this case, the camera was equipped with an infrared lighting system and an infrared filter. The camera was calibrated observing the calibration grid, in order to measure the displacements and the rotations in physical coordinates. The position of the roller meter was coincident with the walkway axis (maximum error smaller than 2 mm); a scheme of the measurement method is shown in Figure 4.

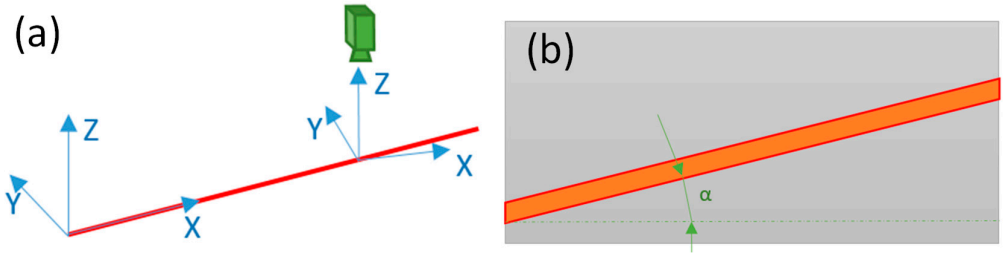


**Figure 4**: Scheme of the system for the measurement of the cart yaw (a) and extraction of the yaw angle from the image (b)

The yaw angle is measured by a custom edge detection algorithm: the grayscale levels image is divided into columns (5 pixels wide). Data of each column is processed using a moving average performed on a 15 x 5 pixels window. All the points in which the grey-scale level variation is larger than 10 are used for the edge detection; the cart yaw angle is measured by fitting the points in a least square sense. The slope is bounded between ±5° and the region of interest for the calculation the threshold is limited to 20 rows above or below the one computed at the previous step; these values

Peer-reviewed version available at Machines 2017, 5, 32; doi:10.3390/machines5040032



were chosen after the analysis of the maximum yaw in operative conditions. With this approach, the image processing time is approximately 15 ms.

A similar system has been used also for the measurement of the pitch angle. The reference line is the walkway handrail, and the edge used for the identification of the pitch is the one between the handrail and the background. Starting from the top of the image, the derivative of the intensity has been computed on the image averaged on a 5 x 5 window. Preliminary analyses showed that with the proposed experimental setup the edge is the best line fitting the points exceeding the level of 20 grayscale units/pixel. The angle is constrained between ±9°. The region of interest for the calculation of this line is limited to 80 pixels above or below the previously calculated line. The image processing time is approximately 30 ms. Examples of the images used for the identification of the cart pitch and yaw are shown in Figure 5.

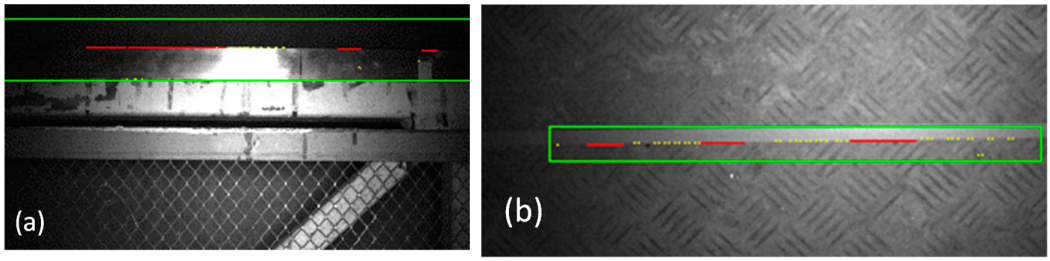


**Figure 5**: Pictures for the identification of the car yaw (a) and pitch (b).

*2.2. System calibration and Uncertainty Budget*

The system calibration is necessary for both the transformation of the images coordinates into physical coordinates (camera calibration) and for the compensation of the bias errors due to the non-idealities of the measurement system (system calibration). The camera calibration was performed by acquiring the image of the calibration grid and compensated for the perspective and nonlinear (optical) distortions of the cameras; the standard nonlinear compensation algorithm of LabVIEW was used in all the analyses.

The system calibration procedure included the experimental evaluation of the measurement uncertainty and the compensation of the bias errors [20-23]. The latter were significant only in the "laser spot and cameras" subsystem, where the lasers' misalignment results in a drift of the cart position and a linearly increasing roll angle. The calibration was performed by comparing the tilt measured by the laser spots and camera to that measured by a reference inclinometer (dual axis SEIKA SBG2U, full-scale ±10° and linearity deviation lower than 0.01°) at different distances (from 1 to 10 m). The error due to the laser misalignment was derived by plotting the difference between the angle measured by the inclinometer and that measured by the vision system as a function of the distance. The linear component of the trend (approximately 2° after 10 meters in our prototype) was subtracted from the measurements performed in operative conditions; as later discussed, the error is large because of the limited quality of the optical setup but does not limit the method accuracy given that, being repeatable, can be compensated.

The uncertainties of the different components of the measurement chain were evaluated as the standard deviation measured in repeatability conditions (given that all the systematic errors outlined in the calibration are compensated). Uncertainty of the laser distance meter was verified at distances of 2.5, 5, 10 and 15 m. Tests results evidenced a standard uncertainty of 0.3 mm.

Uncertainty of the displacements measured by the cameras were evaluated under repeatability conditions, i.e. by observing the spots and edges when the cart was not moving. Uncertainty of the displacement measurement performed by the laser spot and vision system was 0.1 mm, which corresponded to 1/5 of the pixel size (0.5 mm). The resulting uncertainty of the yaw angle is 0.04°.

The uncertainty of pitch and yaw angles was measured by imposing known rotations of ± 5° to an aluminum profile and using the edge detection algorithms described in this paper. The standard uncertainty was 0.03°; this value is probably an underestimation of the value that can be obtained in

operating conditions, since the background during the edge detection did not varied during the calibration tests. Furthermore, the algorithm starts from the assumption that the edge to be detected is an ideal line, and in the current method implementation, the lack of linearity of the edge results in a reduction of the method accuracy. The summary of the uncertainties reported in this section are summarized in Table 1.

**Table 1**: Summary of the uncertainties obtained with the proposed method

| Quantity | Uncertainty |
|---|---|
| Displacement x (motion) | 0.3 mm |
| Displacement y (lateral) | 0.1 mm |
| Displacement z (vertical) | 0.1 mm |
| roll | 0.03° |
| pitch | 0.03° |
| yaw | 0.04° |

### *2.3. Laser scanner boresight*

The laser scanner (Faro 3D) boresight calibration consists in finding the roto-translation between the Laser reference system and the cart reference system, as seen in the upper part of Figure 6. The transformation is obtain by scanning a set of 4 nonaligned markers set fixed on the cart with the laser scanner mounted on the cart and with another laser scanner that observes the cart with the markers.

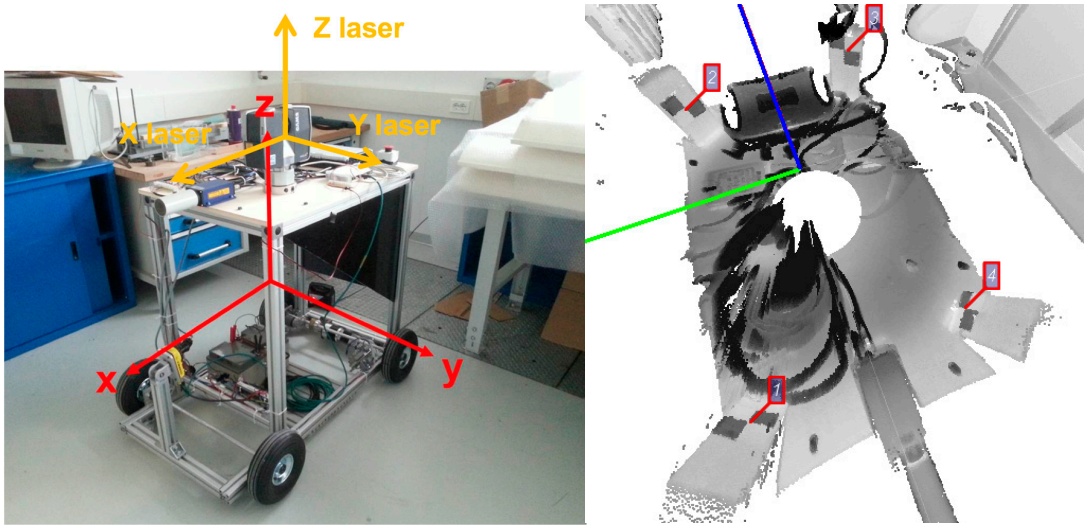


**Figure 6:** Laser Scanner reference systems on the cart (left) and 3D scan of the set of 4 markers located on the cart (as seen from the laser scanner, right)

An example of a 360° view acquired by the FARO laser scanner located on the cart is shown in Figure 8.

Preprints (www.preprints.org) | NOT PEER-REVIEWED | Posted: 27 October 2017 doi:10.20944/preprints201710.0172.v1

Peer-reviewed version available at Machines 2017, 5, 32; doi:10.3390/machines5040032



**Figure 7:** 360° view of the scan performed in GEXCEL laboratories

## 3. Results

The system (cart + laser scanner) has been used for acquiring a known geometry of two environments: i) an indoor corridor and ii) external facade. In both the cases, the geometry of the two environments has been reconstructed by the Faro 3D laser scanner located on the moving cart (mobile acquisition) was compared to the geometry measured by the same Faro laser scanner placed in a fixed position (tripod/static acquisition) along the corridor respectively and at the center of the façade. The error of the proposed method was quantified by creating a reference mesh (triangulated model) out from the static scan, and calculating the distance between the reference triangle and the closer 3D point acquired in the mobile mode. The results of the inspection procedure performed indoor are shown in Figure 8.

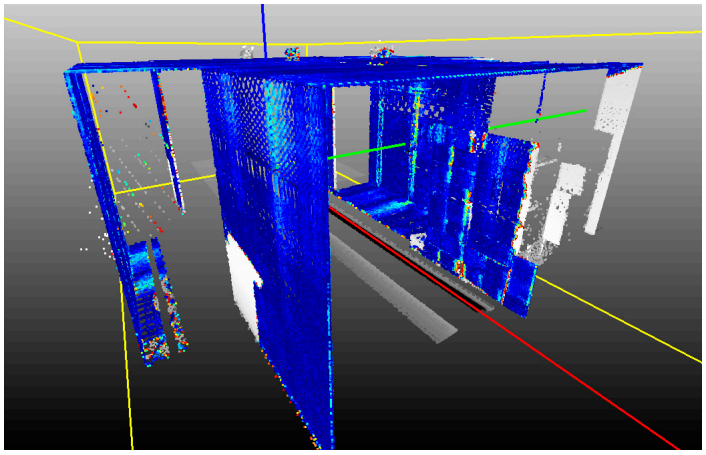

**Figure 8:** Reconstruction of the corridor

Results in the reconstruction of the corridor geometry are summarized in Figure 9 (that shows the corridor observed from above). The plot shows that the errors are generally smaller than 4 mm; as the value is obtained with a regular ground surface and in controlled light conditions, larger values are expected in real tests.

Preprints (www.preprints.org) | NOT PEER-REVIEWED | Posted: 27 October 2017 doi:10.20944/preprints201710.0172.v1

Peer-reviewed version available at Machines 2017, 5, 32; doi:10.3390/machines5040032



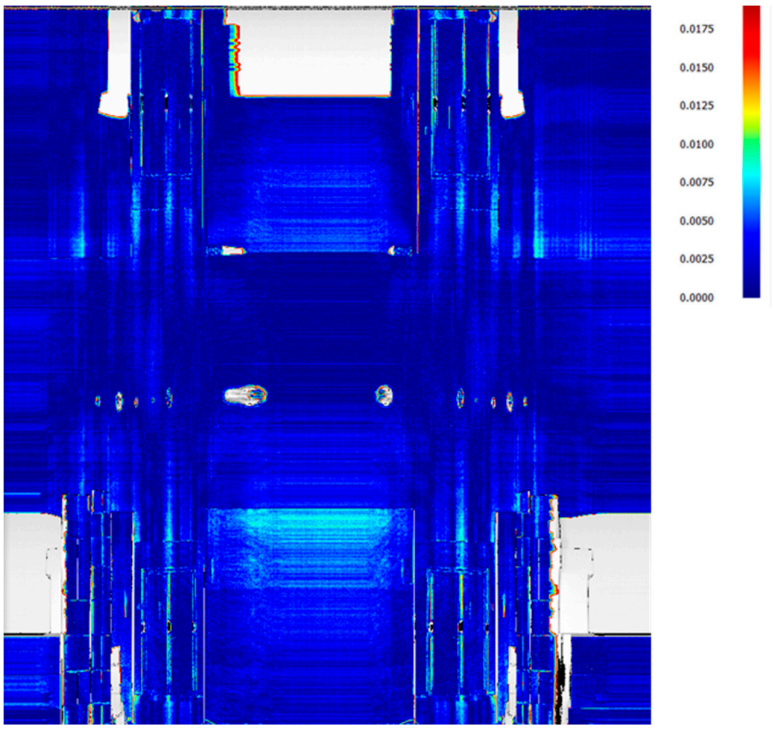


**Figure 9:** 2D map extracted from the 3D reconstruction of the corridor

The second series of tests was performed outdoor in conditions that are more similar to those expected under the bridges; the setup for the method validation is shown in Figure 10. The Faro 3D scanning head was mounted on the instrumented cart moving forth and back over a non-flat terrain simulating the by-bridge. A roller meter was fixed on the ground and two linear metal rods (lateral rails) were fixed on a fence. The cart moved for approximately 15 m and then returned to its original position. The cart nominal speed was 1.2 m/s, a value 20% larger than the ideal speed identified by imposing a point density of 1600 points /dm² with the resolution set to ¼ (helical scans rate 95 Hz).

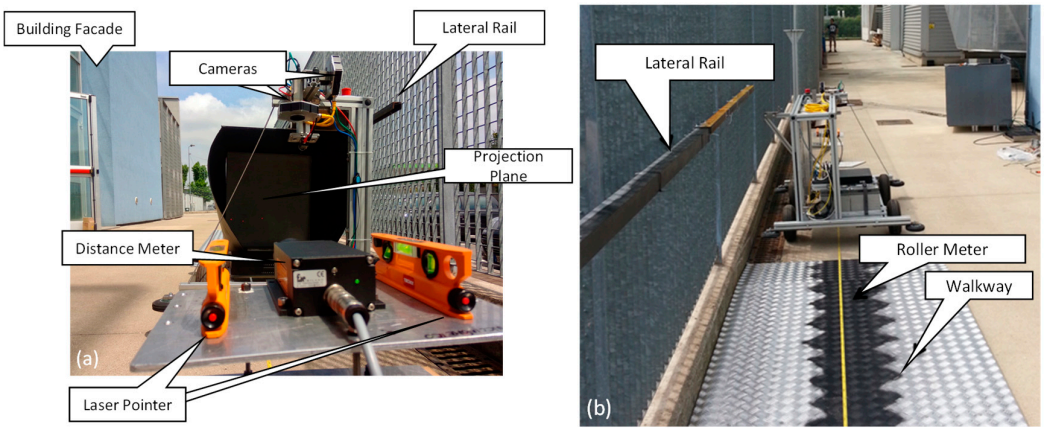


**Figure 10:** Pictorial views of the experimental setup used for the method validation

Successively, the planarity error of the facade was evaluated as the difference the static and the mobile acquisitions. Results are summarized in Figure 11, that shows the cloud of point obtained before the tilt compensation (part a and b) and after the compensation (part c) of all the systematic errors. One can notice that the progressive twist of the façade is recovered after the laser misalignment compensation. The RMS value of the error (distance between static and dynamic scan) was lower than 6 mm; the error increased on the higher part of the façade and was constant at

different distances from the measurement origin (position of the laser pointers). The possible causes of the planarity error evidenced in this section, the method limitations and the possible improvements are discussed in section 4.

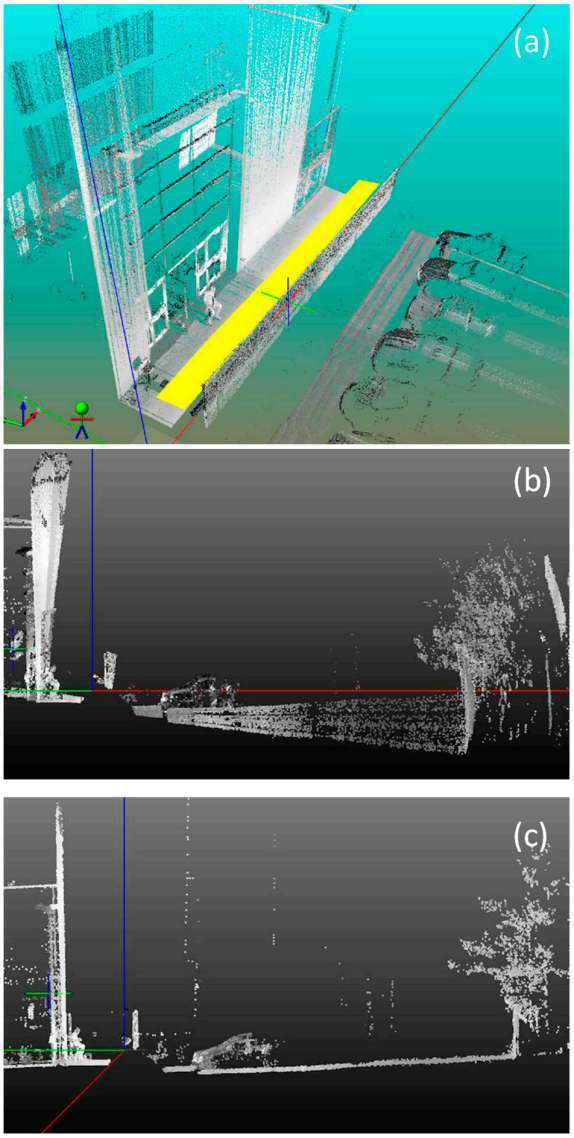


**Figure 11:** Images of the facade reconstructed by the moving cart without the lasers misalignment compensation (a and b) and after the misalignment compensation (c).

## 4. Discussion

Results evidenced that the RMS error of the observed building façade (6 mm outside, less than 4 mm inside) is compatible with that of the methods existing in the literature [24]. The uncertainty is large in comparison with the uncertainty of the cart position, and numerical simulations [18] evidenced that the error is mainly due to a combination of tilt error of the cart and large distance between the cart and the observed surface (3 to 10 m). The position error increases linearly with the distance between the scanning head and the measured surface. In real experimental conditions the error is supposed to be smaller as the distance from the bridge surface is lower than 2 m. In the real by-bridge usage, the accuracy can be increased by considering only the points placed at a limited distance from the scanning head, given that the simultaneous cart and truck motion allows observing the same point from different cart/truck positions.

The accuracy of the angles' measurements can be increased by improving the image quality. The increase of image resolution is not possible since (without increasing significantly the instrumentation cost) this choice would limit the camera framerate and consequently the cart speed (that strongly affects the cart vibration [1,2]). The uncertainty of the edge detection algorithms can be reduced by increasing the contrast between the edges and the background; consequently the tests in actual working conditions were performed by painting the walkway surface of a special opaque paint, as shown in the lower part of Figure 10.

Given that the most limiting factor is the accuracy of the roll angle, the latter could be increased by adopting a procedure similar to the one used to measure the pitch and yaw angles, i.e. by replacing the two laser pointers with a laser line. In order to obtain a decent contrast with the projection plane, the laser aperture should be large enough to fill the entire projection plane at the smaller distance (approximately 1 m) and should have enough power to ensure a sufficient contrast at the distance of 20 m. A similar result can be obtained by replacing the two laser pointers with an array of pointers and adopting a least square procedure to identify the roll angle with a better accuracy. With our experimental setup, the parallelism of the three lasers was limited by the poor planarity of the optical bench and the usage of 3 lasers instead of the external ones did not increase the measurement accuracy significantly.

Also the position uncertainty can be reduced by adopting data fusion procedures [25-27], given that the lateral and vertical displacements can be detected by the vertical and lateral cameras respectively and the odometry can be performed by analyzing the images of the vertical camera (which observes the roller meter). The theoretical uncertainty reduction in case of average of two measures with similar uncertainty is $\sqrt{2}$ [28,29]; however, the increase of accuracy in the final application (reconstruction of the underbridge geometry) would be limited, given that the angles can be measured only by one camera at a time.

Many limitations of the proposed measurement system for the identification of the bridge geometry derive from the odd surface on which the cart is moving and the easiest solution would be ensuring a smoother motion of the cart. For obvious safety reasons it is impossible to modify the structure of the walkway, that is telescopic and can be folded on the truck during the transport phase. Since the by-bridge is used for ordinary road maintenance, the non-slip aluminum on the floor is often in poor conditions, and the telescopic structure of the walkway prevents the use of linear guides (rails) that would ensure a limited roll, pitch and yaw of the cart.

The results presented in this paper evidenced that the mechanical design of the entire structure can be optimized by increasing the quality of the optical bench and by modifying the design of the cart, introducing passive or active suspension systems in order to limit the vibration of the 3D scanning head. These improvements are deserved to forthcoming studies, given that the accuracy of 6 mm on a 15 by 10 meters surface was judged sufficient for the identification of macroscopic structural damages.

## 5. Conclusions

This paper described an original technique for the identification of the motion of a moving cart on bounded trajectories. The proposed solution is based on a simple optical system; after the drift compensation, the accuracy does not increase with the distance of the cart from the origin and the method is therefore convenient for the reconstruction of the underbridge geometry. Results showed that the uncertainty of the position is approximately 0.3 mm in the direction of motion of the cart and close to 0.1 mm in the lateral and vertical directions. The uncertainty of the tilt angles, after the compensation of the linear guides' misalignment, was lower than 0.05°. The proposed method can be used in any application where it is necessary to identify the position of an object along a quasi-rectilinear path and the accuracy can be increased by using cameras with larger resolution and by adopting high quality laser pointers/ laser distance meters. The method validation was eventually performed mounting a 3D laser scanner on a cart moving forth and back on a non-flat surface. The RMS error in the reconstruction of a corridor structure and of a building façade (15 by 10 meters)

were respectively 4 and 6 mm; the values are promising for the final application of the system, given that it was obtained with the cart moving at a speed 20% larger than the actual one.

**Acknowledgments:** Authors gratefully acknowledge SINECO SPA for the financial support of this activity.

**Author Contributions:** Hermes Giberti and Federico Cheli conceived the method. Remo Sala designed the experiments. Silvio Giancola, Hermes Giberti and Marco Tarabini performed the experiments. Marco Tarabini and Hermes Giberti analyzed the data. The paper was written by Marco Tarabini and Silvio Giancola.

**Conflicts of Interest:** The authors declare no conflict of interest

## References

1. Zanoni, A.; Maninetti, G.; Cheli, F.; Garozzo, M. Development of a Computer Vision Tracking System for Automated 3D Reconstruction of Concrete Bridges, ASME 2014 12th Biennial Conference on Engineering Systems Design and Analysis, American Society of Mechanical Engineers: 2014; , pp. V003T15A012-V003T15A012.
2. Giberti, H.; Zanoni, A.; Mauri, M.; Gammino, M. Preliminary study on automated concrete bridge inspection, ASME 2014 12th Biennial Conference on Engineering Systems Design and Analysis, American Society of Mechanical Engineers: 2014; , pp. V003T15A011-V003T15A011.
3. McCrea, A.; Chamberlain, D.; Navon, R. Automated inspection and restoration of steel bridges—a critical review of methods and enabling technologies. *Autom Constr* **2002**, *11*, 351-373.
4. Hugenschmidt, J. Concrete bridge inspection with a mobile GPR system. *Constr Build Mater* **2002**, *16*, 147-154.
5. Adhikari, R.; Moselhi, O.; Bagchi, A. Image-based retrieval of concrete crack properties for bridge inspection. *Autom Constr* **2014**, *39*, 180-194.
6. Busca, G.; Cigada, A.; Mazzoleni, P.; Tarabini, M.; Zappa, E. Static and dynamic monitoring of bridges by means of vision-based measuring system, Conference Proceedings of the Society for Experimental Mechanics Series, 2013; , pp. 83-92.
7. Yu, S.; Jang, J.; Han, C. Auto inspection system using a mobile robot for detecting concrete cracks in a tunnel. *Autom Constr* **2007**, *16*, 255-261.
8. Brilakis, I.; Fathi, H.; Rashidi, A. Progressive 3D reconstruction of infrastructure with videogrammetry. *Autom Constr* **2011**, *20*, 884-895.
9. Zhu, Z.; German, S.; Brilakis, I. Detection of large-scale concrete columns for automated bridge inspection. *Autom Constr* **2010**, *19*, 1047-1055.
10. Abudayyeh, O.; Al Bataineh, M.; Abdel-Qader, I. An imaging data model for concrete bridge inspection. *Adv Eng Software* **2004**, *35*, 473-480.
11. Nistér, D.; Naroditsky, O.; Bergen, J. Visual odometry, Computer Vision and Pattern Recognition, 2004. CVPR 2004. Proceedings of the 2004 IEEE Computer Society Conference on, IEEE: 2004; , pp. I-652-I-659 Vol. 1.
12. Stein, G.P.; Mano, O.; Shashua, A. A robust method for computing vehicle ego-motion, Intelligent Vehicles Symposium, 2000. IV 2000. Proceedings of the IEEE, IEEE: 2000; , pp. 362-368.

13. Rolland, J.P.; Davis, L.; Baillot, Y. A survey of tracking technology for virtual environments. *Fundamentals of wearable computers and augmented reality* **2001**, *1*, 67-112.
14. Portugal-Zambrano, C.E.; Mena-Chalco, J.P. Robust range finder through a laser pointer and a webcam. *Electronic Notes in Theoretical Computer Science* **2011**, *281*, 143-157.
15. Scaramuzza, D.; Fraundorfer, F. Visual odometry [tutorial]. *Robotics & Automation Magazine, IEEE* **2011**, *18*, 80-92.
16. Moravec, H.P. *Obstacle avoidance and navigation in the real world by a seeing robot rover*. **1980**.
17. Giancola, S.; Giberti, H.; Sala, R.; Tarabini, M.; Cheli, F.; Garozzo, M. A non-contact optical technique for vehicle tracking along bounded trajectories. *JOURNAL OF PHYSICS CONFERENCE SERIES* **2015**, 1-13.
18. Giberti, H.; Tarabini, M.; Cheli, F.; Garozzo, M. Accuracy Enhancement Of A Device For Automated Underbridge Inspections, IMAC XXXIV, A Conference and Exposition on Structural Dynamics, , Orlando, Florida2016; .
19. Fossati, F.; Sala, R.; Basso, A.; Rocchi, M.G.D. A multicamera displacement measurement system for wind engineering testing. *FLORENCE ITALY JULY 19t h-23r d* , 217.
20. Moschioni, G.; Saggin, B.; Tarabini, M.; Hald, J.; Morkholt, J. Use of design of experiments and Monte Carlo method for instruments optimal design. *Meas J Int Meas Confed* **2013**, *46*, 976-984.
21. Joint Committee for Guides in Metrology (JCGM) GUIDE 98-3/suppl.1:2008 Evaluation of measurement data - Supplement 1 to the Guide to the expression of uncertainty in measurement - Propagation of distributions using a Monte Carlo method. **2008**.
22. Tarabini, M.; Saggin, B.; Scaccabarozzi, D.; Moschioni, G. The potential of micro-electro-mechanical accelerometers in human vibration measurements. *J Sound Vibrat* **2012**, *331*, 487.
23. Bich, W.; Cox, M.G.; Harris, P.M. Evolution of the ' Guide to the Expression of Uncertainty in Measurement '. *Metrologia* **2006**, *43*, S161.
24. Müller, M.; Surmann, H.; Pervölz, K.; May, S. The accuracy of 6D SLAM using the AIS 3D laser scanner, Multisensor Fusion and Integration for Intelligent Systems, 2006 IEEE International Conference on, IEEE: 2006; , pp. 389-394.
25. Hall, D.L.; Llinas, J. An introduction to multisensor data fusion. *Proceedings of the IEEE* **1997**, *85*, 6-23.
26. Taniguchi, M.; Tresp, V. Averaging regularized estimators. *Neural Comput* **1997**, *9*, 1163-1178.
27. Ferrari, D.; Giberti, H. A genetic algorithm approach to the kinematic synthesis of a 6-DoF parallel manipulator, Control Applications (CCA), 2014 IEEE Conference on, IEEE: 2014; , pp. 222-227.
28. Moschioni, G.; Saggin, B.; Tarabini, M. 3-D Sound Intensity Measurements: Accuracy Enhancements With Virtual-Instrument-Based Technology. *Instrumentation and Measurement, IEEE Transactions on* **2008**, *57*, 1820-1829.

29. Silvestri, M.; Confalonieri, M.; Ferrario, A. Piezoelectric actuators for micro positioning stages in automated machines: experimental characterization of open loop implementations. *FME Transactions* **2017***, 45*, 331-338.